The Linnean Society of London
BIOLOGICAL Journal of the Linnean Society

Evidence of introgressive hybridization between the morphologically divergent land snails Ainohelix and Ezohelix

Journal:	*Biological Journal of the Linnean Society*
Manuscript ID:	BJLS-3696.R1
Manuscript Type:	Research Article
Date Submitted by the Author:	28-Nov-2014
Complete List of Authors:	Morii, Yuta; Tohoku University, Graduate School of Life Sciences Yokoyama, Jun; Yamagata University, Department of Biology Kawata, Masakado; Tohoku University, Graduate School of Life Sciences Davison, Angus; University of Nottingham, Centre for Genetics and Genomics Chiba, Satoshi; Tohoku University, Graduate School of Life Sciences
Keywords:	land snail, Bradybaenidae, phylogeny, morphology, introgression, ancestral hybridization

TITLE

Evidence of introgressive hybridization between the morphologically divergent land snails *Ainohelix* and *Ezohelix*.

Running heads

Introgressive hybridization between land snail species

Author names and institutions

Yuta Morii[1]*, Jun Yokoyama[2], Masakado Kawata[1], Angus Davison[3], Satoshi Chiba[1]

[1] Graduate School of Life Sciences, Tohoku University, Sendai, Miyagi 980-8576, Japan

[2] Department of Biology, Faculty of Science, Yamagata University, Kojirakawa, Yamagata 990-8560, Japan

[3] Centre for Genetics and Genomics, School of Life Sciences, University of Nottingham, Nottingham NG7 2RD, UK

***Corresponding author**

E-mail address: iiromatuy@gmail.com (Y. Morii)

ABSTRACT

Hybridization between different taxa is likely to take place when adaptive morphological differences evolve more rapidly than reproductive isolation. In studying the phylogenetic relationship between two land snails of different nominal genera, *Ainohelix editha* and *Ezohelix gainesi* from Hokkaido, Japan, using nuclear ITS (nDNA) and mitochondrial 16S ribosomal DNA (mtDNA), we found a marked incongruence in the topology between nuclear and mitochondrial phylogenies. Furthermore, no clear association was found between shell morphology (which defines the taxonomy) and nuclear or mitochondrial trees and morphology of reproductive system. These patterns are most likely explained by historical introgressive hybridization between *A. editha* and *E. gainesi*. As the shell morphologies of the two species are quite distinct, even when they coexist, the implication is that natural selection is able to maintain (or has recreated) distinct morphologies in the face of gene flow. Future studies may be able to reveal the regions of the genome that maintain the morphological differences between these species.

ADDITIONAL KEYWORDS: land snail - Bradybaenidae - phylogeny - morphology - introgression - ancestral hybridization

INTRODUCTION

The means by which phenotypic evolution is associated with speciation and genetic differentiation has been a major concern of evolutionary biology (Schluter, 2000; Gavrilets & Losos, 2009), with the general perception being that morphological divergence should reflect the underlying taxonomy and thus the genetic divergence between different species (Avise, 2000; Schileyko, 2004). However, a range of recent studies has uncovered molecular genetic evidence that is suggestive of hybridization and introgression between species with quite divergent morphologies (Rieseberg *et al*., 2003; Seehausen, 2004; Arnold, 2006; Whitney *et al*., 2010; Keller *et al*., 2013; Parham *et al*., 2013). This is probably because phenotypic divergence under natural selection, or even drift, might sometimes take place much faster than the evolution of reproductive isolation, and thus speciation (Teshima *et al*., 2003; Nosil, 2012; Stankowski, 2013). In addition, it has been argued that novel adaptations sometimes arise via hybridization (DeVicente & Tanksley, 1993; Cosse *et al*., 1995; Rieseberg *et al*., 1999; Chiba, 2005; Whitney *et al*., 2010). However, the extent to which interspecific hybridization affects morphological diversity and phenotypic adaptation is unclear, with a few notable exceptions (Whitney *et al*., 2006; Rieseberg, 2011; Pardo-Diaz *et al*., 2012). This is partly because introgressive hybridization is often cryptic (Mallet, 2005; Good *et al*., 2008), and only revealed from combined nuclear and mitochondrial studies (Arnold, 2006; Parham *et al*., 2013).

Land snails are potentially excellent systems to test theories of morphological evolution, because shell shape and colour, both inherited characters, tend to evolve rapidly (Chiba, 1999; Davison & Chiba, 2006; Hoso *et al.*, 2010; Stankowski, 2011, 2013). In this study, we focused on some species of the bradybaenid land snail in Hokkaido and Honshu, Japan. *Ainohelix* and *Ezohelix* are endemic to Japan, and include single species (*Ainohelix editha* and *Ezohelix gainesi*, respectively). Both species have large variations in morphological traits among local populations, and they included many nominal species as synonyms (Habe, 1977;

Minato, 1988; Katakura *et al*., 1990; Teshima *et al*., 2003). *Paraegista* is also endemic to Japan, and includes two described species, *Paraegista takahidei* and *P. apoiensis*. Another native bradybaenid genus, *Karaftohelix* is widely distributed in the northeastern parts of Asian continent, Sakhalin Island, Kuril Islands and Hokkaido Island. Only *Karaftohelix blakeana*, is distributed in Hokkaido (Habe, 1977; Minato, 1988; Schileyko, 2004). Because of clear discontinuities of shell morphological traits, these species have been thought to be quite distinct and distantly related, so these species were classified into four different genera in total (*Ainohelix*, *Ezohelix*, *Karaftohelix* and *Paraegista*). However, a previous molecular phylogenetic study suggested that three genera (*Ainohelix*, *Ezohelix* and *Paraegista*) were genetically close to one other (Wade *et al*., 2006), perhaps calling into question the generic status. A prior molecular phylogenetic analysis of *A. editha* suggested that morphological divergence of *A. editha* may have occurred independently in different lineages (Teshima *et al*., 2003). However, no molecular surveys have been conducted in other land snail genera of Hokkaido.

In the present study, we clarified the phylogenetic relationships among all Japanese species of *Ainohelix*, *Ezohelix*, *Karaftohelix* and *Paraegista* altogether, using nuclear internal transcribed spacer DNA (*ITS1* and *ITS2*, nDNA) and mitochondrial *16S* ribosomal DNA (mtDNA) genetic markers. In particular, we aimed to understand how the topology of phylogenetic trees inferred from nDNA compares with that of mtDNA, and whether either or both are associated with the shell and genital morphological traits of two morphologically divergent land snails of *Ainohelix editha* and *Ezohelix gainesi*. The genital morphology is often used as taxonomically important trait for terrestrial molluscs (Schileyko, 2004). Causes of incongruence among the gene trees and phenotypic traits and observed evolutionary patterns are discussed.

MATERIAL AND METHODS

Samples

Ainohelix editha (Figure 1a,b) is a widely distributed endemic species of Hokkaido Island. Two different morphs have been identified in the populations of *A. editha*. The keeled morph is characterized by having a peripheral angle on the shell, and the rounded morph by having no pheripheral angle. The keeled morph is found only in the populations from Urakawa (Samani, locality no.48) and Shimamaki (Obira, locality no.45), though intermediate morphs between rounded and keeled morphs are found (Teshima *et al*., 2003). *Ezohelix gainesi* (Figure 1c) is also found on Hokkaido, as well as high mountains in the Tohoku region of Honshu Island. Snail samples of these species were collected from 57 localities covering almost the entire distributional range (Figure 2; Appendix 1). The three remaining bradybaenid species of Hokkaido were also sampled, *Karaftohelix blakeana* (Figure 1d), *Paraegista takahidei* (Figure 1e) and *Paraegista apoiensis* (Figure 1f). These three species have limited distributions on Hokkaido (Japan Wildlife Research Center, 2002).

A previous phylogenetic study sampled three of the four bradybaenid genera, *Ezohelix*, *Ainohelix* and *Paraegista*, putting them in a single monophyletic group (Wade *et al*., 2006). As we were primarily interested in the relationship between *Ezohelix* and *Ainohelix*, we used *P. apoiensis* from Samani (locality no. 52) as an outgroup for phylogenetic analyses.

A fragment of the foot muscle of each individual was stored in 100% ethanol for DNA extraction, and the other parts of the soft tissue of each individual were stored in 70% ethanol after dissecting and observing the morphology of the reproductive system.

Molecular methods

Foot tissue was homogenized in 300 µl cetyltrimethylammonium bromide (CTAB) solution [2% CTAB (w/v), 100 mM Tris (pH 8.0), 20 mM EDTA (pH 8.0), 1.4M NaCl] and 20 µL of 10 mg/mL proteinase K, incubated at 60 °C for approximately 1 hour, extracted once with phenol/chloroform and precipitated with two volumes of ethanol. The DNA pellet was then

rinsed with 70% ethanol, vacuum-dried for approximately 1 hour and dissolved in 50 µL of distilled water.

Approximately 1200 bp of a nuclear gene cluster (nDNA), including the complete ITS-1 region (approximately 530 bp), the complete 5.8S gene (approximately 160 bp), and the complete ITS-2 region (approximately 480 bp) was amplified by PCR, using six primers, ITS1 (5'-TCC GTA GGT GAA CCT GCG G-3'; White *et al*., 1990), ITS3 (5'-GCA TCG ATG AAG AAC GCA GC-3'; White *et al*., 1990), ITS4 (5'-TCC TCC GCT TAT TGA TAT GC-3'; White *et al*., 1990), ITS5 (5'-GGA AGT AAA AGT CGT AAC AAG G-3'; White *et al*., 1990), ITSsq2 (5'-CAC ACG ATA GGA AGC GAT TG-3'; original) and ITSsq4 (5'-ATG CTT AAA TTC AGC GGG TA-3'; original). Similarly, approximately 900 bp of the mitochondrial 16S ribosomal DNA (mtDNA) was also amplified by PCR, using four primers, 16Scs1 (5'-AAA CAT ACC TTT TGC ATA ATG G-3'; Chiba, 1999), 16Scs2 (5'-AGA AAC TGA CCT GGC TTA CG-3'; Chiba, 1999), 16SinnerF2 (5'-TAC TCT GAC TGT GCA AAG GTA G-3'; original) and 16SinnerR (5'-GGG TCT TCT CGT CTA TTA TTT A-3'; original). Both PCR reactions were conducted using Takara rTaq™ (Takara Biomedicals, Japan) and buffers. Thermal cycling was performed with following reaction conditions: 94°C for 1 min., followed by 40 cycles of 94 °C for 1 min, 50 °C for 1 min and 72 °C for 1 min, with final extension at 72 °C for 7 min. Cycle sequencing was carried out with both forward and reverse primers, using ~80-100 ng of PCR product in the reaction and the BigDye™ Terminator v3.0 Cycle Sequencing Ready Reaction Kit (Applied Biosystems, California). DNA sequences were electrophoresed on a 310 Genetic Analyser or 3130 Genetic Analyser (both Applied Biosystems, California).

Phylogenetic analyses

In total, 123 and 185 individuals of the five species including the outgroup taxa were used for nDNA and mtDNA analyses, respectively. Sequences were aligned using Clustal W (Thompson *et al*., 1994), and results were then checked manually to minimize the total

number of insertions and deletions (indels). All indel sites were removed from the alignment before phylogenetic analyses. The SH test (Shimodaira & Hasegawa, 1999) and approximately unbiased (AU) test (Shimodaira, 2002) were conducted using 114 individuals that have both nDNA and mtDNA sequences (Appendix 1). Gene trees were constructed using Bayesian inference (BI) methods and maximum likelihood (ML) methods with nDNA and mtDNA datasets analyzed separately, because SH test (Shimodaira & Hasegawa, 1999) and approximately unbiased (AU) test (Shimodaira, 2002) showed that the two datasets contained significantly different phylogenetic information. These analyses were conducted using TREEFINDER (Jobb et al., 2004) based on the selected 114 individuals that have both nDNA and mtDNA sequences (Appendix 1). Each dataset was treated as a single gene region for phylogenetic analyses. A GTR + Gamma model was selected according to the Akaike's information criterion (AIC; Akaike, 1974) for both nDNA and mtDNA datasets.

BI analyses were carried out using KAKUSAN v4.0 (Tanabe, 2007) and MrBayes v3.1.2 (Huelsenbeck & Ronquist, 2001). Tree space was explored using two concurrent runs with four simultaneous Markov Chain Monte Carlo (MCMC) chains for 10 million generations, sampling every 1000 generations. The number of generations before stationarity of likelihood values was estimated, with the aid of the value of mean standard deviation of split frequencies in MrBayes (the value became less than 0.01; Huelsenback & Ronquist, 2001) and TRACER v1.5 (the effective sample sizes of all parameters became more than 100 after the burn-in; Rambaut & Drummond, 2007). The heating parameters were set to 0.15. After discarding the first 10001 trees as burn-in, we obtained the 50% majority rule consensus tree and the posterior probabilities of nodes in the tree.

ML analyses were carried out using KAKUSAN v4.0 (Tanabe, 2007) and TREEFINDER (Jobb *et al*., 2004). Rate heterogeneity between sites was accounted for by Gamma distributed rates (Yang, 1994) in the model. The confidence level of the nodes in the ML tree was estimated using bootstrap resampling (Felsenstein, 1985) on 1000 pseudoreplicates.

Haplotype networks were constructed using using TCS v2.1 (Clement, 2000).

Morphological analyses

A shell morphological analysis was conducted for *A. editha* and *E. gainesi* (78 and 37 specimens, respectively) from 25 sites (Appendix 1). Four shell morphological characters, aperture height (AH), aperture width (AW), shell diameter (D), shell height (H), were measured using a digital vernier caliper (Niigataseiki, Japan) and the number of coils was counted by 1/4 whorls (Figure 3a). The lengths of these traits were measured through comparison with a scale of ±0.1 mm accuracy. The mean of the three measurements for each trait was used for the analyses. A principal component analysis (PCA) was conducted on the correlation matrix of log-transformed measurements using JMP software (SAS Institute, North Carolina).

An analysis of reproductive system was also conducted for *A. editha* and *E. gainesi* (38 and 19 specimens, respectively) from 17 sites (Appendix 1). Nine morphological characters of the reproductive system were measured on the pictures of reproductive system using ImageJ software (National Institutes of Health, Bethesda, USA; Figure 3b): length of stalk of the bursa copulatrix (Lbc), length between the upper end of the penis sheath and the retractor muscle of the penis (Lep1), length between the upper end of the epiphallus and the retractor muscle of the penis (Lep2; i.e. length of epiphallus = Lep1+Lep2), length of oviduct (Lov), length of the penis (Lps), length of the spermoviduct (Lsd), Length of stylophore or dart sac (Lst), length of the vagina (Lva), length of the vas deferens (Lvd). A principal component analysis (PCA) was conducted using the ratio of the length of each character to the length from the genital apex to the tip of the epiphallus was calculated in JMP software (SAS Institute, North Carolina).

RESULTS

Phylogenetic analyses

We did not concatenate the nDNA and mtDNA sequences because the SH test (Shimodaira & Hasegawa, 1999) and approximately unbiased (AU) test (Shimodaira, 2002) suggested that the two data sets contain significantly different phylogenetic information (P <0.001 on both tests).

nDNA variations

In the nDNA analyses, BI and ML (a single tree with -ln L 3155.) analyses did not result in identical topologies, especially for the phylogenetic position of clade E. The topology of the haplotype network was consistent with the topology of BI tree (Appendix 2). Therefore, ML tree was not used for subsequent analyses. The inferred phylogenetic relationship among the haplotypes is shown in Figure 4.

There were no shared haplotypes between *A. editha* and *E. gainesi*. *A. editha* and *E. gainesi* were polyphyletic, with the majority of *E. gainesi* haplotypes falling into three clades, A, C and E, with high support values (BPP = 0.86, 1.00 and 1.00, BV = 82%, 92% and 96%, respectively), except for two haplotypes from three populations (locality no. 7, 15 and 49). The haplotype network suggested that *E. gainesi* were derived from more than two genetically distinctive clades (Clades A+C and E, Appendix1). Although the phylogenetic relationships between many haplotypes of *A. editha* were uncertain, three clades, B, D and F, were identified by high support values (BPP = 0.96, 0.97 and 1.00, BV = 83%, 70% and 84%, respectively). The haplotypes included in each of these six clades were those from geographically close populations, but each clade does not overlap geographically with others in most cases (Figure 5). The two populations of keeled morph of *A. editha* were included in the different clades respectively (Clade F and uncertain clade).

mtDNA variations

In the mtDNA analyses, 185 individuals of five species, including the outgroup taxa, were

analyzed, detecting 127 haplotypes. The BI and ML resulted in nearly identical topologies. The ML analysis resulted in a single tree with -lnL 9323.59. The inferred phylogenetic relationship among the haplotypes is shown in Figure 6.

Similarly to the nDNA analyses, *A. editha* and *E. gainesi*, were polyphyletic in the mtDNA analyses, with no shared haplotypes between the two species. Six major clades were identified (Clades G-L). Clade G included haplotypes of both *A. editha* and *E. gainesi* (97 haplotypes), and occupied the largest geographic area among the six clades, encompassing almost the entire distribution of these two species. The other clades (Clades H-L) tended to include either *A. editha* or *E. gainesi* (Figure 6).

Clade G was separated into 10 well supported subclades (Subclades G1-10). These five clades (Clade H-L) and 10 subclades (Subclades G1-10) were constructed with the haplotypes of geographically close populations (Figure 7). In particular, G-1 and G-2 clades contain *A. editha* and *E. gainesi*, with the haplotypes being from geographically close sites (Figure 7a,b). The two populations of keeled morph of *A. editha* were included in the different clades respectively (Clade H and Subclade G-2).

Morphological analyses

To investigate variation in shell morphology between *A. editha* and *E. gainesi*, PCA was performed based on five traits (four measurements in Figure 3a and number of whorls). More than 98% of the variation among the individual snails was explained by two principal components (PC1 and PC2; Table 1). All factors had a sufficient loading value, and the factors, except for the number of whorls, had positive loadings on PC1. Therefore, PC1 can be interpreted as explaining both size and shape of the shell.

The difference in the PC1 scores is highly significant between *A. editha* and *E. gainesi* (Wilcoxon rank sum test, $P < 0.001$). *A. editha* was much smaller and coiled more than *E. gainesi*, and there were no intermediate shell types between *A. editha* and *E. gainesi* (Figure 8a). On the basis of PCA, the keeled morph of *A. editha* (white triangles in Figure 8a) was

not clearly sepalated from the rounded morph, as shown in a previous study (Teshima *et al*., 2003).

Similarly, a PCA analysis was performed to investigate variation in genital morphology between *A. editha* and *E. gainesi* based on nine measurements (Figure 3b). In contradiction to the shell morphology, no differences in morphology of reproductive system were distinguishable between the two species, which completely overlapped (Figure 8b).

DISCUSSION

Phylogenetic relationships among bradybaenid snails in Hokkaido

The evidence from the nDNA and mtDNA analyses suggests that five bradybaenid endemic species of Hokkaido and Honshu, *A. gainesi*, *E. editha*, *K. blakeana*, *P. takahidei* and *P. apoiensis* are genetically close to each other. On the basis of both nDNA and mtDNA trees, the populations of *K. blakeana* is monophyletic (Figure 4, 6). In addition, individuals of this species are morphologically close to each other (data not shown), showing that *K. blakeana* is clearly discriminated from *A. editha* and *E. gainesi*. However, populations of *A. editha* and *E. gainesi* show polyphyletic relationships in nDNA and mtDNA analyses (Figure 4, 6). In addition, the *A. editha* and *E. gainesi* are indistinguishable by genital morphologies (Figure 8b). These results indicate that *A. editha* and *E. gainesi* are genetically and anatomically indistinguishably close to each other despite that these species belong to different nominal genera because of their distantly related shell morphologies (Figure 8a). Shell morphologies of land snails are highly labile (Chiba, 1999; Teshima *et al*., 2003; Stankowski, 2011, 2013; Hirano *et al*., 2014), and therefore, *E. gainesi* taxonomically belongs to *Ainohelix*.

The evolutionary histories of *Ainohelix editha* and *Ezohelix gainesi*

Despite absence of differentiation in characters that are usually key for taxonomic description (e.g. morphology of reproductive system), we argue that *A. editha* and *E. gainesi* are nonetheless good species, because the shell size and shape are distinct and often coexist at the same place (30 localities of all 54 sites in this study contained both *A. editha* or *E. gainesi*). In addition, there were no shared haplotypes/alleles between *A. editha* and *E. gainesi*, therefore the reproductive isolation between *A. editha* and *E. gainesi* is likely to be established.

An array of recent molecular phylogenetic studies suggest that introgression of mtDNA tends to occur much more frequently than nuclear DNA (Ferris *et al*., 1983; Taylor & McPhail, 2000; Sota & Vogler, 2001; Doiron *et al*., 2002; Shaw, 2002; Ballard & Whitlock,

2004; Roca *et al*., 2005), although the reasons for this are still unclear (Llopart *et al.*, 2005; Bachtrog *et al*., 2006). In our study, the phylogenetic relationship between *A. editha* and *E. gainesi* appears more complex in mtDNA analyses than in nDNA analyses, although for both genes *A. editha* and *E. gainesi* tend to have very different lineages (Figure 9), suggesting at least a recent separate history. This pattern may suggest that the introgressive hybridization between *A. editha* and *E. gainesi* has occurred during the history of evolution of these species. The geographic patterns of G-1 and G-2 clades of the mtDNA tree including haplotypes of both *A. editha* and *E. gainesi* also strongly suggest a history of introgressive hybridization between *A. editha* and *E. gainesi*.

As alternative hypotheses, the observed patterns could have been produced by incomplete lineage sorting or differential retention of some ancestral polymorphism that was present in the ancestor to these two species (Bull, 1993; Sang & Zhong, 2000; Holder *et al*., 2001; Joly *et al*., 2009). The phylogenetic relationship among the mtDNA haplotypes included in G-1 and G-2 clades does not reflect difference of the species but reflects geographical closeness, suggesting that the observed patterns are difficult to explain with these hypotheses. However, the phylogenetic relationships among other clades of the mtDNA tree may be explained by not only introgressive hybridization but also the incomplete lineage sorting and/or retention of some ancestral polymorphism, because there is no relationship between genetic and geographic structure among clades or subclades.

In the nDNA analyses, the alleles of *E. gainesi* were clearly separated into three clades (A, C and E clades). The haplotype network based on the same nDNA dataset using minimum spanning network showed that the three clades of *E. gainesi* were derived from one clade of *A. editha* independently (Appendix 2). This may imply that *E. gainesi* has evolved three times independently by parallel evolution. Parallel evolution of similar traits in different populations experiencing ecologically similar environments strongly implicates natural selection as the cause of evolution (Hervey & Pagel, 1991; Schluter & Nagel, 1995; Rundle

et al., 2000; Schluter, 2000, 2001; Nosil *et al*., 2002). However, we argue that this parallel pattern of *E. gainesi* in nDNA is unlikely to be caused by parallel evolution, because the geographic patterns of A, C and E clades are not correlated with the geographic history of Hokkaido Island (Yonekura *et al*., 2001). It is possible that the observed phylogenetic patterns were created through multiple mechanisms of the introgressive hybridization, the incomplete lineage sorting with parallel evolution and/or differential retention of ancestral polymorphism. Clearly, further research is needed to clarify the causes of the observed phylogenetic patterns.

As sympatric snails tend to have a discrete morphology and size, as well as there being no evidence of shared haplotypes, we argue that the incongruence of nDNA and mtDNA trees is most likely to be caused by ancestral hybridization. Similar patterns observed in the present study have been reported in several studies (DeSalle & Giddings, 1986; Bagley & Gall, 1998; Wilson & Bernatchez, 1998; Llopart *et al*., 2005; Roca *et al*., 2005; Bachtrog *et al*., 2006; Haase & Misof, 2009; Haase *et al*., 2013). Furthermore, as snails in different regions of Hokkaido tend to have different shared histories, this is probably evidence for geographically discrete hybridization events, perhaps strongly influenced by Pleistocene climate change (Yonekura *et al*., 2001; Koizumi *et al*., 2012). If population sizes were much smaller than today, it is likely that morphologically well differentiated snails mated in Pleistocene isolation but no longer afterwards (Haase & Misof, 2009; Haase *et al*., 2013). Because the mtDNA tree remained the influence of ancestral hybridization between *A. editha* and *E. gainesi*, despite mtDNA have a rapid evolutionaly rate and short coalescence times (Avise, 2000), and *A. editha* and *E. gainesi* can be distinguished clearly and significantly by difference of shell size and shape, therefore it seems possible that the divergence of morphology and speciation of *A. editha* and *E. gainesi* occurred recently, or now is occurring.

Correlations between shell size and moisture have been reported in land snails (larger snails in wetter condition; Goodfriend, 1986). In such cases, mosaic patterns should appear in

the distributions of the two species because of mosaic distributions of these habitats (Futuyma, 2005). However, in unpublished work, we have found no obvious differences in the local microhabitat use between the two species when sympatric, so it is unlikely that morphological differences between the two species are caused by major differences in habitat. Probably, strong selection against intermediate form causes morphological divergence and the two distinctive forms have evolved after hybridization, but further research is needed to clarify the ecological or genetic factors that decrease fitness of intermediate forms.

ACKNOWLEDGEMENTS

We thank Mr. M. Komazawa for providing advice about the collecting materials. We also thank Dr. J. Nekola and an anonymous reviewer for their helpful comments. This study was partly supported financially by Tohoku University's Global Center of Excellence (COE) program, "Ecosystem Adaptability Science for the Future" (no. J03) and a Research Fellowship for Young Scientists from the Japan Society for the Promotion of Science to Y. Morii.

REFERENCES

Akaike H. 1974. A new look at the statistical identification model. *IEEE Transactions on Automatic Control* **19:** 716-723.

Arnold ML. 2006. *Evolution through genetic exchange*. New York: Oxford University Press.

Avise JC. 2000. *Phylogeography, The history and formation of species*. Cambridge, MA: Harvard University Press.

Bachtrog D, Thornton K, Clark A, Andolfatto P. 2006. Extensive introgression of mitochondrial DNA relative to nuclear genes in the *Drosophila yakuba* species group. *Evolution* **60:** 292-302.

Bagley MJ, Gall GAE. 1998. Mitochondrial and nuclear DNA sequence variability among populations of rainbow trout (*Oncorhynchus mykiss*). *Molecular Ecology* **7:** 945-961.

Ballard JWO, Whitlock MC. 2004. The incomplete natural history of mitochondria. *Molecular Ecology* **13:** 729-744.

Bull JJ, Huelsenbeck JH,Cunningham CW, Swofford DL, Waddell PJ. 1993. Partitioningand combining data in phylogenetic analysis. *Systematic Biology* **42:** 384-397.

Chiba S. 1999. Accelerated evolution of land snails *Mandarina* in the oceanic Bonin Islands: Evidence from mitochondrial DNA sequences. *Evolution* **53:** 460-471.

Chiba S. 2005. Appearance of morphological novelty in a hybrid zone between two species of land snail. *Evolution* **59:** 1712-1720.

Clement M, Posada D, Crandall KA. 2000. TCS: a computer program to estimate gene genealogies. *Molecular Ecology* **9:** 1657-1659.

Cosse AA, Campbell MG, Glover, TJ, Linn Jr. CE, Todd JL, Baker TC, Roelofs WL. 1995. Pheromone behavioral responses in unusual male European corn borer hybrid progeny not correlated to electrophysiological phenotypes of their pheromone specific

antennal neurons. *Experientia* **51:** 809-816.

Davison A, Chiba S. 2006. Labile ecotypes accompany rapid cladgenesis in a land snail adaptive radiation. *Biological Journal of the Linnean Society* **88:** 269-282.

DeSalle R, Giddings LV. 1986. Discordance of nuclear and mitochondrial DNA phylogenies in Hawaiian *Drosophila*. *Proceedings of the National Academy of Sciences* **83:** 6902-6906.

DeVicente MC, Tanksley SD. 1993. QTL analysis of transgressive segregation in an interspecific tomato cross. *Genetics* **134:** 585-596.

Doiron S, Bernatchez LB, Pierre UA. 2002. A comparative mitogenomic analysis of the potential adaptive value of Arctic charr mtDNA introgression in brook charr populations (*Salvelinus fontinalis* Mitchill). *Molecular Biology and Evolution* **19:** 1902-1909.

Felsenstein J. 1985. Confidence limits on phylogenies: An approach using the bootstrap. *Evolution* **39:** 783-791.

Ferris SD, Sage RD, Huang CM, Nielsen JT, Ritte U, Wilson AC. 1983. Flow of mitochondrial DNA across a species boundary. *Proceedings of the National Academy of Sciences* **80:** 2290-2294.

Futuyma DJ. 2005. *Evolution.* Sunderland, Massachusetts: Sinauer Associates.

Gavrilets S, Losos JB. 2009. Adaptive radiation: contrasting theory with data. *Science* **323:** 732-737.

Good JM, Hird S, Reid N, Demboski JR, Steppan SJ, Martin-Nims TR, Sullivan J. 2008. Ancient hybridization and mitochondrial capture between two species of chipmunks. *Molecular Ecology* **17:** 1313-1327.

Goodfriend GA. 1986. Variation in land-snail shell form and size and its causes: a review. *Systematic Zoology* **35:** 204-223.

Haase M, Esch S, Misof B. 2013. Local adaptation, refugial isolation and secondary contact of Alpine populations of the land snail *Arianta arbustorum*. *Journal of Molluscan*

Studies **79:** 241-248.

Haase M, Misof B. 2009. Dynamic gastropods: Stable shell polymorphism despite gene flow in the land snail *Arianta arbustorum*. *Journal of Zoological Systematics and Evolutionary Research* **47:** 105-114.

Habe T. 1977. Identity of 'Helix' *blakeana*. Chiribotan **9:** 187-188 (in Japanese).

Harvey PH, Pagel MD. 1991. *The comparative method in evolutionary biology.* Oxford, UK: Oxford University Press.

Hirano T, Kameda Y, Kimura K, Chiba S. 2014. Substantial incongruence among the morphology, taxonomy, and molecular phylogeny of the land snails *Aegista*, Landouria, Trishoplita, and Pseudobuliminus (Pulmonata: Bradybaenidae) occurring in East Asia. *Molecular Phylogenetics and Evolution* **70:** 171-181.

Holder MT, Anderson JA, Holloway AK. 2001. Difficulties in detecting hybridization. *Systematic Biology* **50:** 978-982.

Hoso M, Kameda Y, Wu S, Asami T, Kato M, Hori M. 2010. A speciation gene for left–right reversal in snails results in anti-predator adaptation. *Nature Communications* **1:** 133.

Huelsenbeck JP, Ronquist F. 2001. MrBayes: Bayesian inference of phylogeny. *Bioinformatics* **17:** 754-755.

Japan Wildlife Research Center. 2002. *The national survey on the natural environment report of the distributional survey of Japanese animals (Land and fresh water mollusks).* Tokyo: Biodiversity Center of Japan, Nature Conservation Bureau, Ministry of the Environment.

Jobb G, Haeseler A, Strimmer K. 2004. TREEFINDER: a powerful graphical analysis environment for molecular phylogenetics. *BMC Evolutionary Biology* **4:** 18.

Joly S, McLenachan PA, Lockhart PJ. 2009. A statistical approach for distinguishing hybridization and incomplete lineage sorting. *American Naturalist* **174:** E54-70.

Katakura H, Kuwahara Y, Udagawa T. 1990. Geographical variation of shell morphology in the land snail *Ainohelix editha*: a review of factual evidence. *Journal of Faculty of Science Hokkaido University, Series VI, Zoology* **25:** 118-129.

Keller I, Wagner CE, Greuter L, Mwaiko S, Selz OM, Sibasunder A, Wittwer S, Seehausen O. 2013. Population genomic signatures of divergent adaptation, gene flow and hybrid speciation in the rapid radiation of Lake Victoria cichlid fishes. *Molecular Ecology* **22:** 2848-2863.

Koizumi I, Usio N, Kawai T, Azuma N, Masuda R. 2012. Loss of genetic diversity means loss of geological information: The endangered Japanese Crayfish exhibits remarkable historical footprints. *PLoS ONE* **7:** e33986.

Llopart A, Lachaise D, Coyne JA. 2005. Multilocus analysis of introgression between two sympatric sister species of *Drosophila*: *D. yakuba* and *D. santomea*. *Genetics* **171:** 197-210.

Mallet J. 2005. Hybridization as an invasion of the genome. *TRENDS in Ecology & Evolution* **20:** 229-237.

Mrnato H. 1988. *A systematic and bibliographic list of the Japanese land snails*. Shirahama.

Nosil P, Crespi BJ, Sandoval CP. 2002. Host-plant adaptation drives the parallel evolution of reproductive isolation. *Nature* **417:** 440-443.

Nosil P. 2012. *Ecological Speciation.* New York: Oxford University Press.

Pardo-Diaz C, Salazar C, Baxter SW, Merot C, Figueiredo-Ready W, Joron M, McMillan WO, Jiggins CD. 2012. Adaptive Introgression across Species Boundaries in Heliconius Butterflies. *PLoS Genetics* **8:** e1002752.

Parham JF, Papenfuss TJ, van Dijk PP, Wilson BS, Marte C, Schettino LR, Simison WB. 2013. Genetic introgression and hybridization in Antillean freshwater turtles (Trachemys) revealed by coalescent analyses of mitochondrial and cloned nuclear

markers. *Molecular Phylogenetetics and Evolution* **67:** 176-187.

Rambaut A, Drummond AJ. 2007. "TRACER version 1.5" Software distributed by the author at http://beast.bio.ed.ac.uk/Tracer.

Rieseberg LH. 2011. Adaptive Introgression: The Seeds of Resistance. *Current Biology* **21:** R581-R583.

Rieseberg LH, Archer MA, Wayne RK. 1999. Transgressive segregation, adaptation and speciation. *Heredity* **83:** 363-372.

Rieseberg LH, Raymond O, Rosenthal DM, Lai Z, Livingstone K, Nakazato T, Durphy JL, Schwarzbach AE, Donovan LA, Lexer C. 2003. Major ecological transitions in wild sunflowers facilitated by hybridization. *Science* **301:** 1211-1216.

Roca AL, Georgiadis N, O'Brien SJ. 2005. Cytonuclear genomic dissociation in African elephant species. *Nature Genetics* **37:** 96-100.

Rundle HD, Nagel L, Boughman JW, Schluter D. 2000. Natural selection and parallel speciation in sympatric sticklebacks. *Science* **287:** 306-308.

Seehausen O. 2004. Hybridization and adaptive radiation. *TRENDS in Ecology & Evolution* **19:** 198–207.

Schileyko AA. 2004. *Treatise on recent terrestrial pulmonate molluscs, Part 12: Bradybaenidae, Monadeniidae, Xanthonychidae, Epiphragmophoridae, Helminthoglypridae, Elonidae, Humboldtianidae, Sphincterochilidae, Cochlicellidae.* Moscow: Ruthenica.

Schluter D. 2000. *The ecology of adaptive radiation.* New York: Oxford University Press.

Schluter D. 2001. Ecology and the origin of species. *TRENDS in Ecology and Evolution*, **16:** 372-380.

Schluter D, Nagel LM. 1995. Parallel speciation by natural selection. *The American Naturalist* **146:** 292-301.

Shaw KL. 2002. Conflict between nuclear and mitochondrial DNA phylogenies of a recent

species radiation: what mtDNA reveals and conceals about modes of speciation in Hawaiian crickets. *Proceedings of the National Academy of Sciences* **99:** 16122-16127.

Shimodaira H. 2002. An approximately unbiased test of phylogenetic tree selection. *Systematic Biology* **51:** 492-508.

Shimodaira H, Hasegawa M. 1999. Multiple comparisons of log-likelihoods with applications to phylogenetic inference. *Molecular Biology and Evolution* **16:** 1114-1116.

Sang T, Zhong Y. 2000. Testing hybridization hypotheses based on incongruent gene trees. *Systematic Biology* **49:** 422-434.

Sota T, Vogler AP. 2001. Incongruence of mitochondrial and nuclear gene trees in the carabid beetles *Ohomopterus*. *Systematic Biology* **50:** 39-59.

Stankowski S. 2011. Extreme, continuous variation in an island snail: local diversification and association of shell form with the current environment. *Biological Journal of the Linnean Society* **104:** 756-769.

Stankowski S. 2013. Ecological speciation in an island snail: evidence for the parallel evolution of a novel ecotype and maintenance by ecologically dependent postzygotic isolation. *Molecular Ecology* **22:** 2726-2741.

Taylor EB, McPhail JD. 2000. Historical contingency and ecological determinism interact to prime speciation in sticklebacks, *Proceedings of the Royal Society B: Biological Sciences* **267:** 375-2384.

Teshima H, Davison A, Kuwahara Y, Yokoyama J, Chiba S, Fukuda T, Ogimura H, Kawata M. 2003. The evolution of extreme shell shape variation in the land snail *Ainohelix editha*: a phylogeny and hybrid zone analysis. *Molecular Ecology* **12:** 1869-1878.

Tanabe AS. 2007. KAKUSAN: a computer program to automate the selection of a nucleotide substitution model and the configuration of a mixed model on multilocus data. *Molecular Ecology* **7:** 962-964.

Thompson JD, Higgins DG, Gibson TJ. 1994. CLUSTAL W: improving the sensitivity of progressive multiple sequence alignment through sequence weighting, position specific gap penalties and weight matrix choice. *Nucleic Acids Research* **22:** 4673-4680.

Wade CM, Mordan PB, Naggs F. 2006. Evolutionary relationships among the Pulmonate land snails and slugs (Pulmonata, Stylommatophora). *Biological Journal of the Linnean Society* **87:** 593-610.

White TJ, Bruns T, Lee S, Taylor J. 1990. Amplification and direct sequencing of fungal ribosomal RNA genes for phylogenetics. In *PCR Protocols: A guide to methods and applications.* Edited by Innis MA, Gelfand DH, Shinsky JJ, White TJ. New York: Academic Press: 315-322.

Whitney KD, Ahern JR, Campbell LG, Albert LP, King MS. 2010. Patterns of hybridization in plants. Perspect. *Plant Ecology* **12:** 175-182.

Whitney KD, Randell RA, Rieseberg LH. 2006. Adaptive Introgression of Herbivore Resistance Traits in the Weedy Sunflower *Helianthus annuus*. *American Naturalist* **167:** 794-807.

Wilson CC, Bernatchez L. 1998. The ghost of hybrids past: fixation of arctic charr (*Salvelinus alpinus*) mitochondrial DNA in an introgressed population of lake trout (*S. namaycush*). *Molecular Ecology* **7:** 127-132.

Yang Z. 1994. Maximum likelihood phylogenetic estimation from DNA sequences with variable rates over sites: approximate methods. *Journal of Molecular Evolution* **39:** 306-314.

Yonekura N, Kaizuka S, Nogami M, Chinzei K. 2001. *Regional geomorphology of the Japanese Islands volume 1. Introduction to Japanese geomorphology.* Tokyo: University of Tokyo Press.

FIGURE LEGENDS

Figure 1. Representative specimens of *Ainohelix editha*, *Ezohelix gainesi*, *Karaftohelix blakeana*, *Paraegista takahidei* and *Paraegista apoiensis*. Rounded morph of *A. editha* from Shimamaki (a), keeled morph of *A. editha* from Shimamaki (b), *E. gainesi* from Rumoi (c), *K. blakeana* from Rebun Island (d), *P. takahidei* from Sapporo (e), *P. apoiensis* from Samani (f). All scales indicate 10mm.

Figure 2. Map showing the sampling localities of snails analyzed in this study. The numerals correspond to the locality numbers in Appendix 1.

Figure 3. Characters measured for the morphological analyses of shell (a) and reproductive system (b). AH, aperture height; AW, aperture width; D, shell diameter; H, shell height; Lbc, length of stalk of the bursa copulatrix; Lep1, length between the upper end of the penis sheath and the retractor muscle of the penis; Lep2, length between the upper end of the epiphallus and the retractor muscle of the penis; Lov, length of oviduct; Lps, length of the penis sheath; Lst, length of stylophore or dart sac; Lsd, length of the spermiduct; Lva, length of the vagina; Lvd, length of the vas deferens.

Figure 4. The Bayesian tree inferred from nDNA sequences (approximately 1200bp). Numbers at each branch represent the posterior probability of clades resolved in BI analysis (BPP; values <0.90 are not shown) and bootstrap support for clades resolved in the ML analysis (BV; values <70% are not shown). Numbers at the tips indicate the individual numbers shown in Appendix 1: white circle, *A. editha*; black circle, *E. gainesi*; gray circle, *K. blakeana*; upper gray triangle, *P. takahidei*; lower gray triangle, *P. apoiensis*. The bars on the right side indicate the species included in each clade or subclade: white bar, clade of *A.*

editha; black bar; clade of E. gainesi: gray bar; clade of *K. blakeana*, *P. takahidei* or *P. apoiensis*. Images of typical shell of the individuals belonging to each clade were shown with an asterisk (*) on the image and OTU of the tree.

Figure 5. The geographic relationships among haplotypes in each clade of nDNA tree. Clades of *E. gainesi* (a), clades of *A. editha* (b), other haplotypes that did not construct any clades (c).

Figure 6. The Bayesian tree inferred from mtDNA sequences (approximately 900bp). Numbers at each branch represent the posterior probability of clades resolved in BI analysis (BPP; values <0.90 are not shown) and bootstrap support for clades resolved in the ML analysis (BV; values <70% are not shown). Numbers at the tips indicate the individual numbers shown in Appendix 1: white circle, *A. editha*; black circle, *E. gainesi*; gray circle, *K. blakeana*; upper gray triangle, *P. takahidei*; lower gray triangle, *P. apoiensis*. The bars on the right side indicate the species included in each clade or subclade: white bar, clade or subclade of *A. editha*; black bar, clade or subclade of *E. gainesi*; stripe bar, subclade including both *A. editha* and *E. gainesi*; gray bar, clade of *K. blakeana*, *P. takahidei* or *P. apoiensis*.

Figure 7. The geographic relationships among haplotypes in each clade and subclade of mtDNA tree. Clade G-1 and G-2 were constructed by both haplotypes of *A. editha* and *E. gainesi* (a,b). Other clades included either only *A. editha* (c) or *E. gainesi* (d).

Figure 8. Scatter plots of the principal component scores of shell (a) and reproductive system (b). White circle, rounded morph of *A. editha*; lower white triangle, keeled morph of *A. editha* from Shimamaki (locality no. 45); upper white triangle, keeled morph of *A. editha* from Urakawa (locality no. 48); black circle, *E. gainesi*.

Figure 9. Inconsistency of topology between nDNA tree (left) and mtDNA tree (right). Numbers at the tips indicate the locality numbers shown in Appendix 1. Haplotype possessed by the same individual was connected by a solid line (*E. gainesi*) and broken line (*A. editha*).

TABLES

Table 1. Summary of principal component analysis for the morphological analysis of shells.

measurement	PC1	PC2
Eigenvalue	4.395	0.517
% of total variation	87.903	10.342
Coefficient		
D	0.975	0.091
AW	0.991	0.096
H	0.947	0.274
AH	0.995	0.050
Coils	-0.759	0.650

Table 2. Summary of principal component analysis for the morphological analysis of reproductive system.

measurement	PC1	PC2	PC3	PC4
Eigenvalue	1.932	1.750	1.374	1.126
% of total variation	21.446	19.449	15.271	12.510
Coefficient				
Lbc	0.189	0.205	0.656	0.388
Lep1	0.310	-0.369	0.367	0.327
Lep2	0.635	-0.384	-0.277	-0.210
Lov	-0.483	0.185	0.310	0.284
Lps	0.803	0.040	0.100	-0.018
Lsd	-0.639	-0.640	-0.292	0.103
Lst	-0.327	0.161	0.553	-0.646
Lva	-0.041	0.586	-0.409	0.493
Lvd	0.056	0.781	-0.260	-0.269

APPENDICES

Appendix 1. Sampling information of specimens used in the present study.

Appendix 2. The parsimony haplotype network conducted using the nDNA. Circles (nodes) indicate each haplotype. Numbers in the circles indicate the individual numbers shown in Appendix 1. Connection between nodes indicates a single character-state change. The empty nodes indicate missing haplotypes. Numbers in the nodes indicate the sampling location, and the size of the nodes is proportional to the haplotype's frequency. White and black nodes indicate haplotypes of *Ainohelix editha*, *Ezohelix gainesi*, respectively. Gray nodes indicate the other three species, *Karaftohelix blakeana*, *Paraegista takahidei and P. apoiensis*.

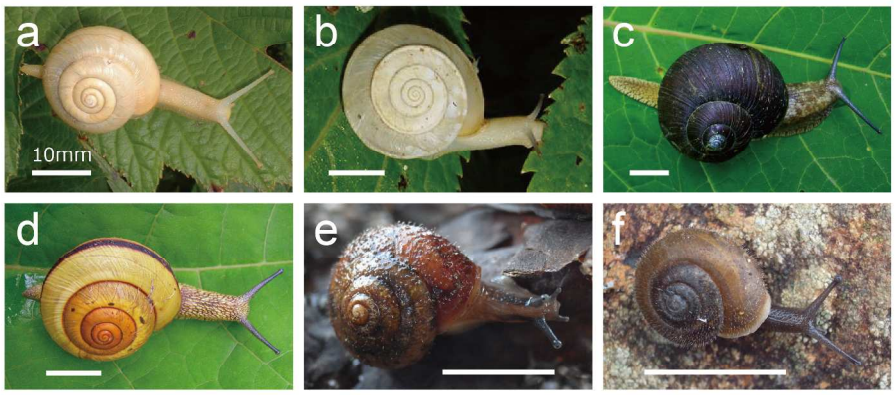

Figure 1. Representative specimens of Ainohelix editha, Ezohelix gainesi, Karaftohelix blakeana, Paraegista takahidei and Paraegista apoiensis. Rounded morph of A. editha from Shimamaki (a), keeled morph of A. editha from Shimamaki (b), E. gainesi from Rumoi (c), K. blakeana from Rebun Island (d), P. takahidei from Sapporo (e), P. apoiensis from Samani (f). All scales indicate 10mm.

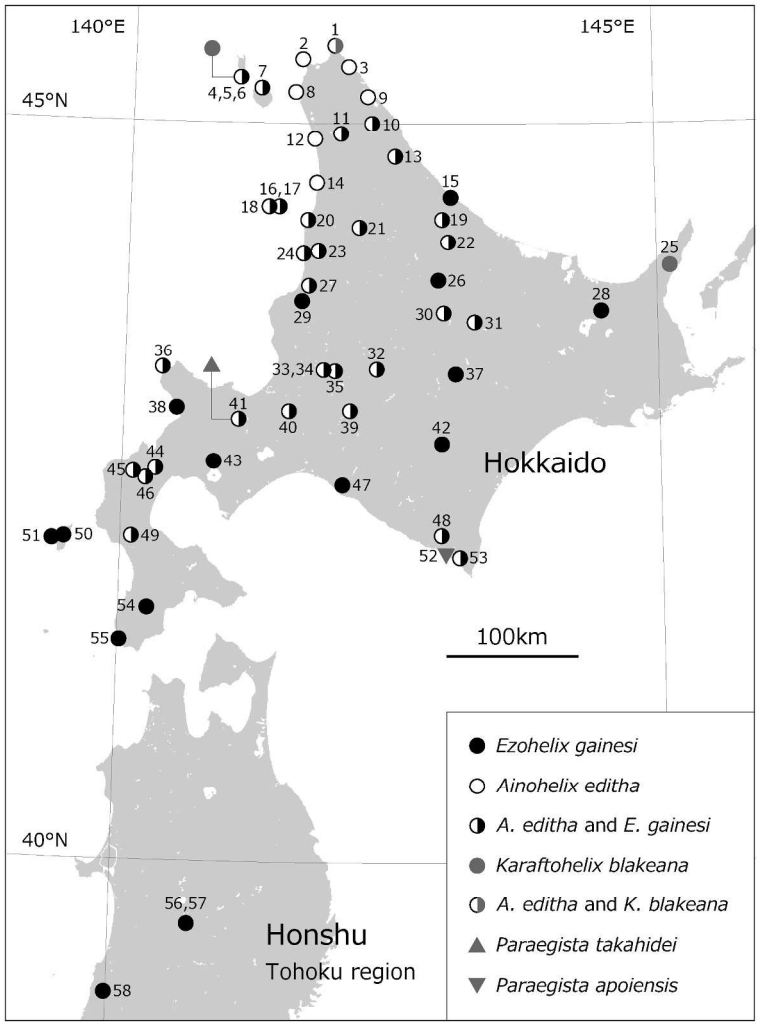

Figure 2. Map showing the sampling localities of snails analyzed in this study. The numerals correspond to the locality numbers in Appendix 1.
215x279mm (300 x 300 DPI)

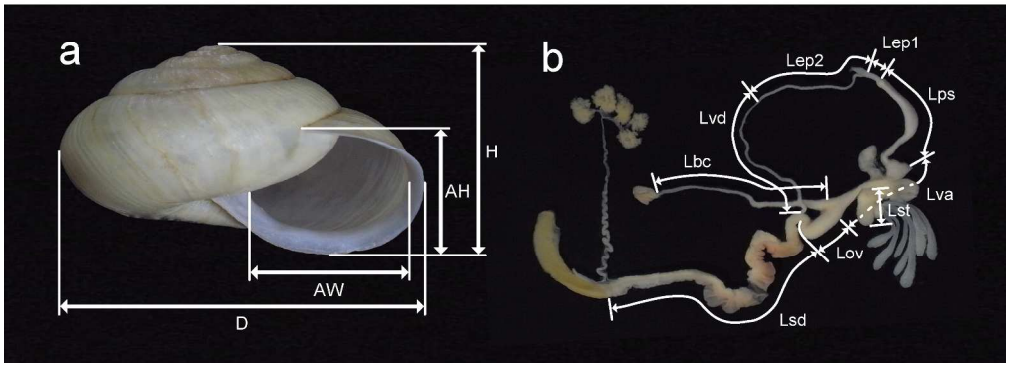

Figure 3. Characters measured for the morphological analyses of shell (a) and reproductive system (b). AH, aperture height; AW, aperture width; D, shell diameter; H, shell height; Lbc, length of stalk of the bursa copulatrix; Lep1, length between the upper end of the penis sheath and the retractor muscle of the penis; Lep2, length between the upper end of the epiphallus and the retractor muscle of the penis; Lov, length of oviduct; Lps, length of the penis sheath; Lst, length of stylophore or dart sac; Lsd, length of the spermiduct; Lva, length of the vagina; Lvd, length of the vas deferens.
282x211mm (300 x 300 DPI)

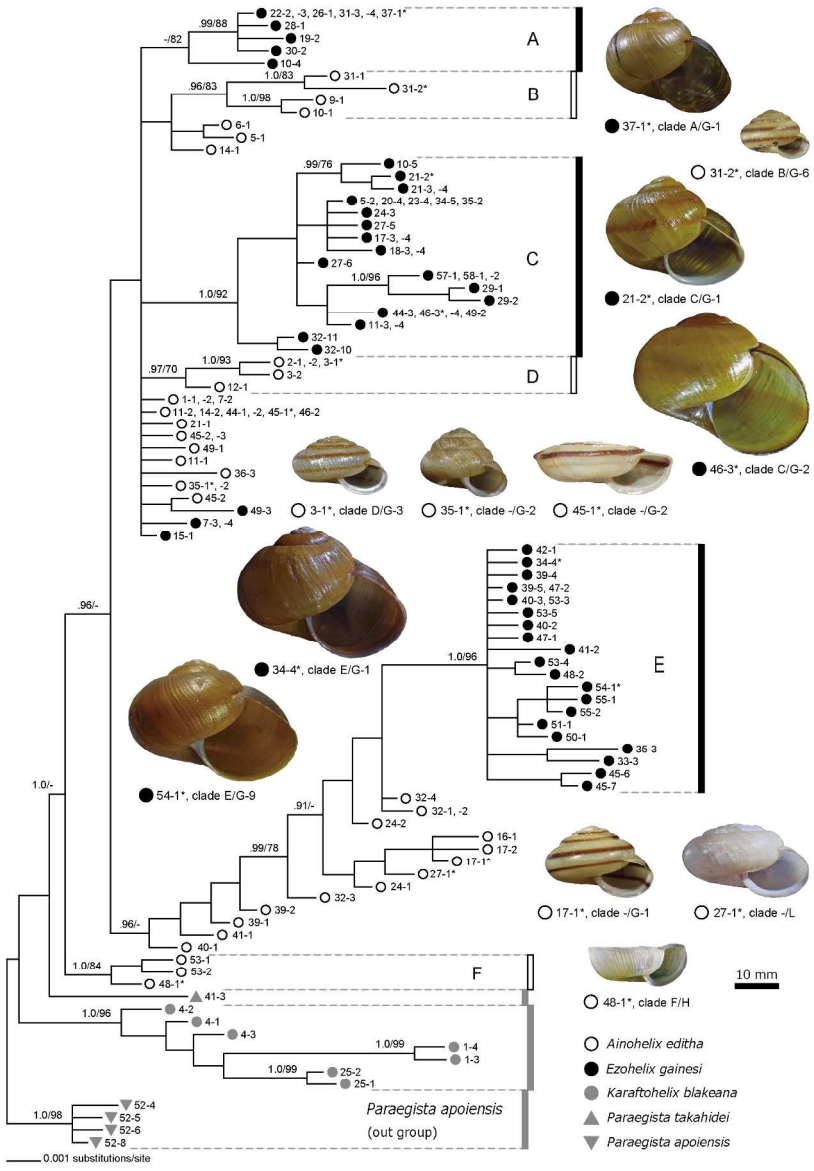

Figure 4. The Bayesian tree inferred from nDNA sequences (approximately 1200bp). Numbers at each branch represent the posterior probability of clades resolved in BI analysis (BPP; values <0.90 are not shown) and bootstrap support for clades resolved in the ML analysis (BV; values <70% are not shown). Numbers at the tips indicate the individual numbers shown in Appendix 1: white circle, A. editha; black circle, E. gainesi; gray circle, K. blakeana; upper gray triangle, P. takahidei; lower gray triangle, P. apoiensis. The bars on the right side indicate the species included in each clade or subclade: white bar, clade of A. editha; black bar; clade of E. gainesi: gray bar; clade of K. blakeana, P. takahidei or P. apoiensis. Images of typical shell of the individuals belonging to each clade were shown with an asterisk (*) on the image and OTU of the tree.
211x282mm (300 x 300 DPI)

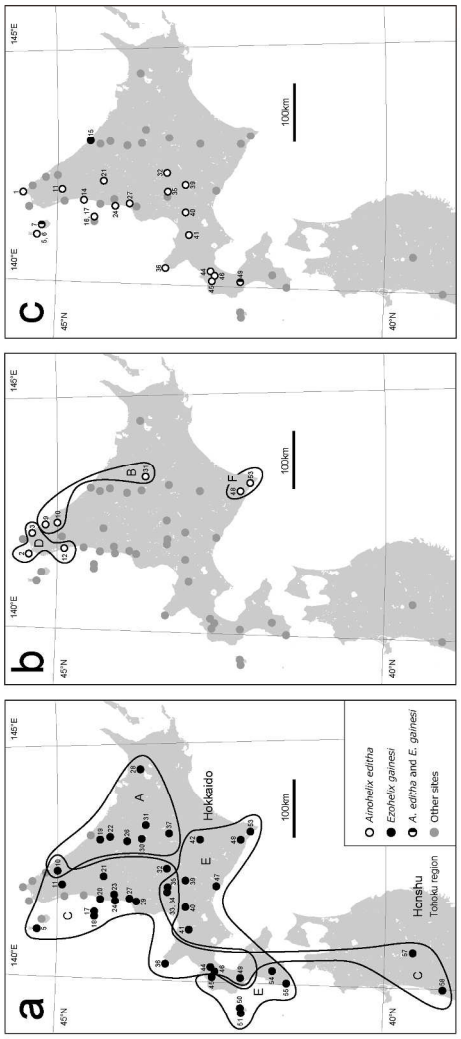

Figure 5. The geographic relationships among haplotypes in each clade of nDNA tree. Clades of E. gainesi (a), clades of A. editha (b), other haplotypes that did not construct any clades (c).
211x282mm (300 x 300 DPI)

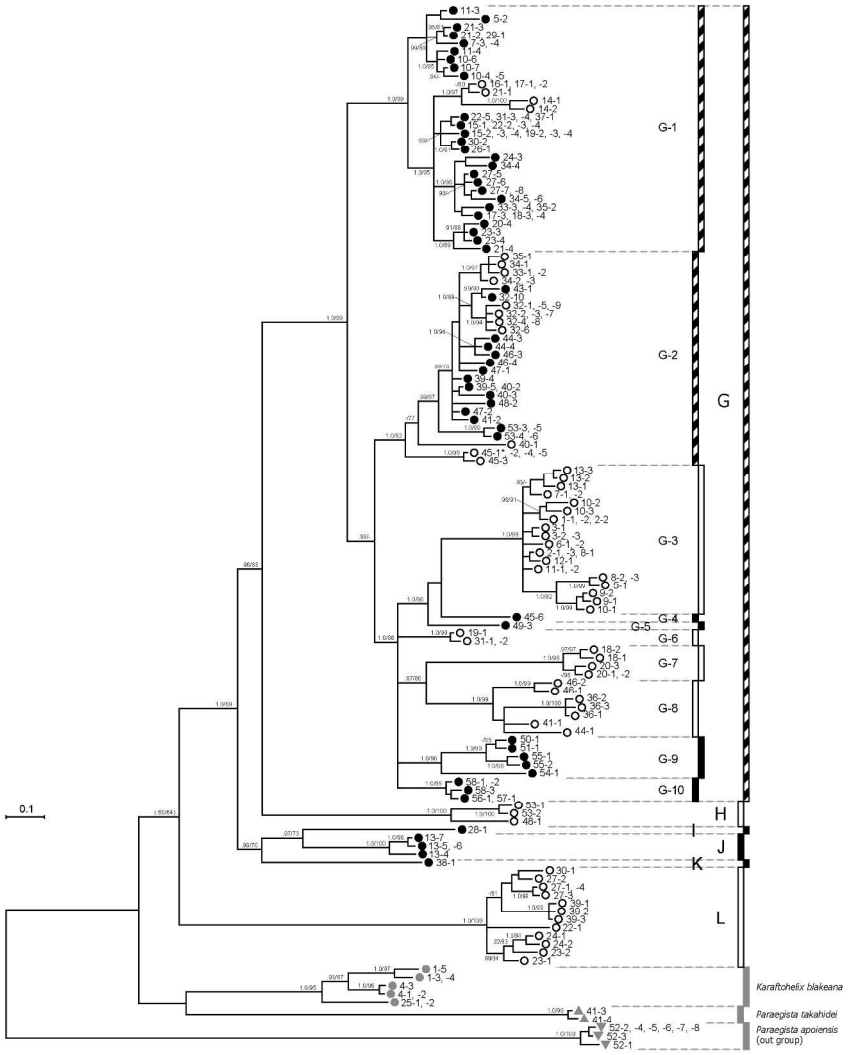

Figure 6. The Bayesian tree inferred from mtDNA sequences (approximately 900bp). Numbers at each branch represent the posterior probability of clades resolved in BI analysis (BPP; values <0.90 are not shown) and bootstrap support for clades resolved in the ML analysis (BV; values <70% are not shown). Numbers at the tips indicate the individual numbers shown in Appendix 1: white circle, A. editha; black circle, E. gainesi; gray circle, K. blakeana; upper gray triangle, P. takahidei; lower gray triangle, P. apoiensis. The bars on the right side indicate the species included in each clade or subclade: white bar, clade or subclade of A. editha; black bar, clade or subclade of E. gainesi; stripe bar, subclade including both A. editha and E. gainesi; gray bar, clade of K. blakeana, P. takahidei or P. apoiensis.
211x282mm (300 x 300 DPI)

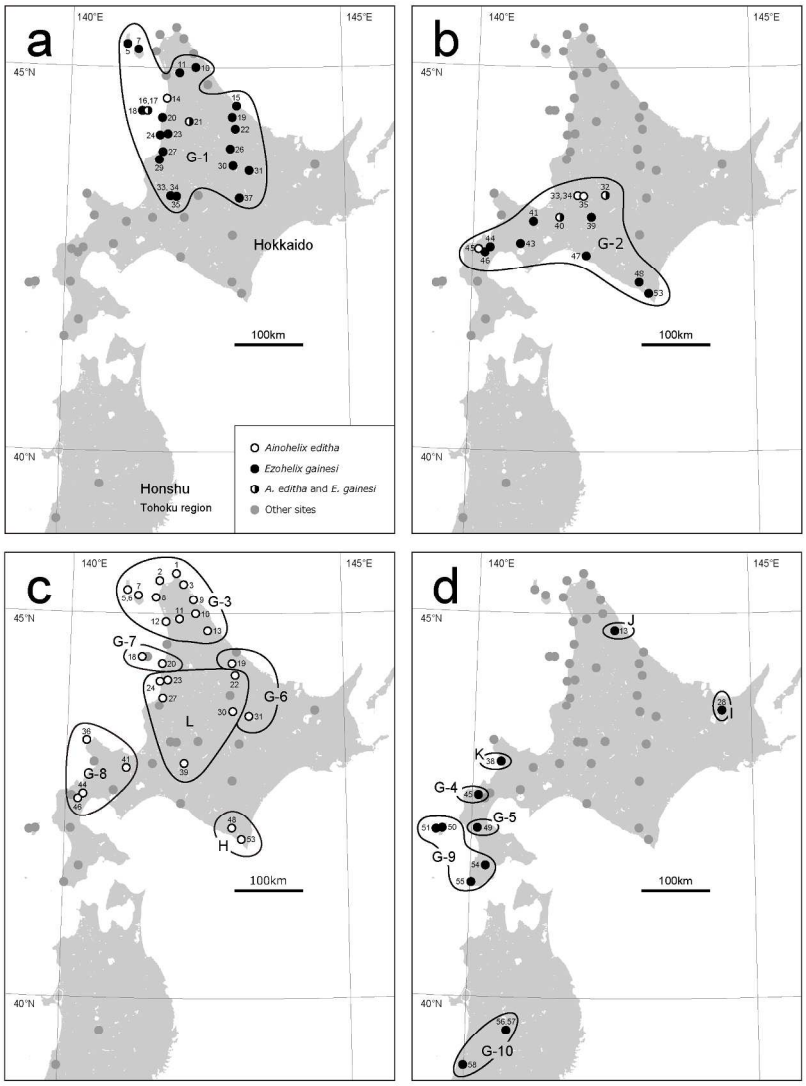

Figure 7. The geographic relationships among haplotypes in each clade and subclade of mtDNA tree. Clade G-1 and G-2 were constructed by both haplotypes of A. editha and E. gainesi (a,b). Other clades included either only A. editha (c) or E. gainesi (d).
215x279mm (300 x 300 DPI)

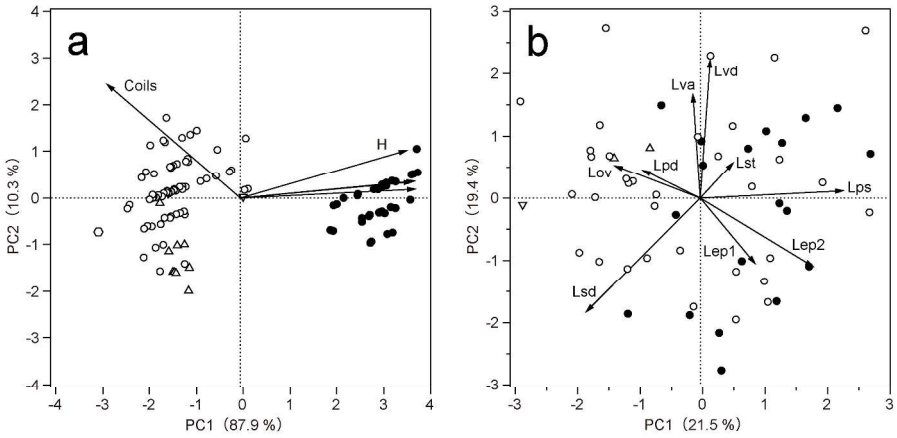

Figure 8. Scatter plots of the principal component scores of shell (a) and reproductive system (b). White circle, rounded morph of A. editha; lower white triangle, keeled morph of A. editha from Shimamaki (locality no. 45); upper white triangle, keeled morph of A. editha from Urakawa (locality no. 48); black circle, E. gainesi.
282x211mm (300 x 300 DPI)

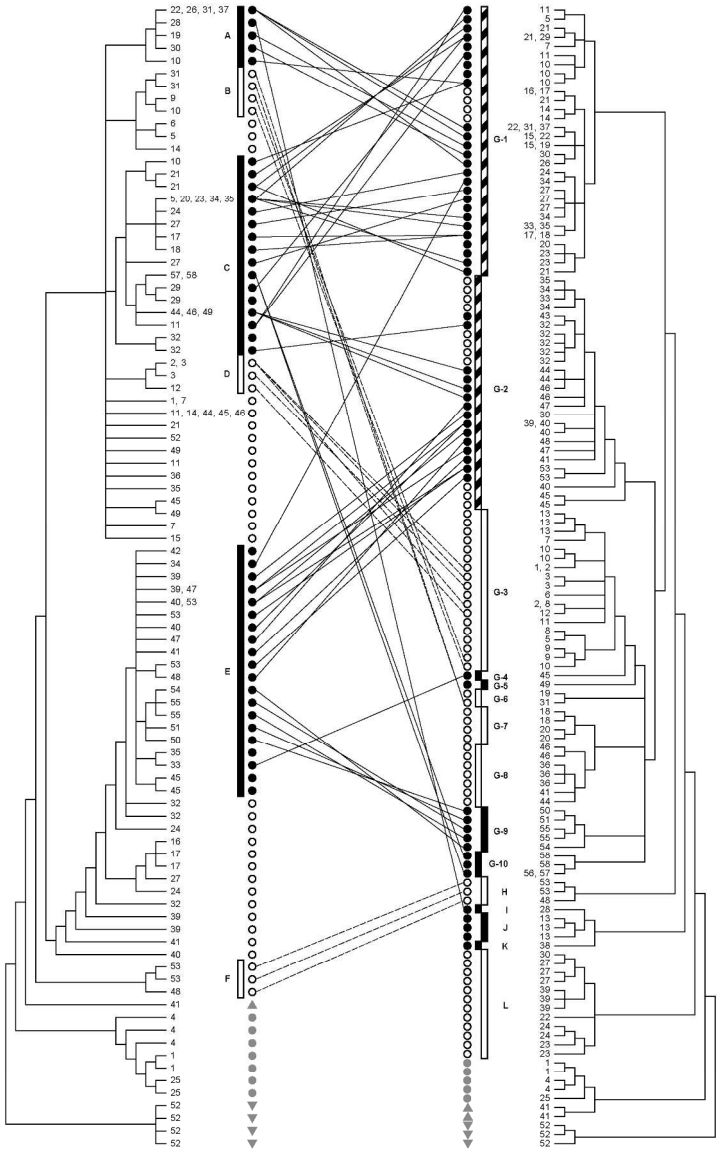

Figure 9. Inconsistency of topology between nDNA tree (left) and mtDNA tree (right). Numbers at the tips indicate the locality numbers shown in Appendix 1. Haplotype possessed by the same individual was connected by a solid line (E. gainesi) and broken line (A. editha).
211x282mm (300 x 300 DPI)

Table 1. Summary of principal component analysis for the morphological analysis of shells.

measurement	PC1	PC2
Eigenvalue	4.395	0.517
% of total variation	87.903	10.342
Coefficient		
D	0.975	0.091
AW	0.991	0.096
H	0.947	0.274
AH	0.995	0.050
Coils	-0.759	0.650

Table 2. Summary of principal component analysis for the morphological analysis of reproductive system.

measurement	PC1	PC2	PC3	PC4
Eigenvalue	1.932	1.750	1.374	1.126
% of total variation	21.446	19.449	15.271	12.510
Coefficient				
Lbc	0.189	0.205	0.656	0.388
Lep1	0.310	-0.369	0.367	0.327
Lep2	0.635	-0.384	-0.277	-0.210
Lov	-0.483	0.185	0.310	0.284
Lps	0.803	0.040	0.100	-0.018
Lsd	-0.639	-0.640	-0.292	0.103
Lst	-0.327	0.161	0.553	-0.646
Lva	-0.041	0.586	-0.409	0.493
Lvd	0.056	0.781	-0.260	-0.269

Appendix 1. Sampling information of specimens used in the present study.

Locality no. and name	Coodinates Latitude/Longitude	Morphology Shell	Genitalia	Molecular Identification ID	ITS	16S
Ainohelix editha						
1 Soya, Wakkanai	45°31′N/141°56′E	-	1	1-1	AB893822	AB893666
				1-2	AB893823	AB893667
2 Wakkanai	45°25′N/141°38′E	-	-	2-1	AB893804	AB893631
				2-2	AB893805	AB893632
				2-3	-	AB893633
3 Sarufutsu	45°22′N/142°05′E	6	-	3-1	AB893799	AB893623
				3-2	AB893800	AB893624
				3-3	-	AB893625
5 Rebun Island	45°18′N/141°02′E	1	-	5-1	AB893803	AB893630
6 Rebun Island	45°17′N/141°01′E	4	-	6-1	AB893802	AB893628
				6-2	-	AB893629
7 Rishiri Island	45°13′N/141°14′E	1	1	7-1	AB893801	AB893627
				7-2	-	AB893626
8 Yurai, Wakkanai	45°12′N/141°35′E	1	-	8-1	-	AB893634
				8-2	-	AB893635
				8-3	-	AB893636
9 Hamatombetsu	45°10′N/142°16′E	-	-	9-1	AB893798	AB893621
				9-2	-	AB893622
10 Nakatombetsu	44°59′N/142°17′E	5	2	10-1	AB893797	AB893618
				10-2	-	AB893619
				10-3	-	AB893620
11 Horonobe	44°55′N/142°00′E	-	-	11-1	AB893831	AB893682
				11-2	AB893832	AB893683
12 Teshio	44°53′N/141°45′E	4	-	12-1	AB893806	AB893637
13 Esashi	44°46′N/142°30′E	1	1	13-1	-	AB893615
				13-2	-	AB893616
				13-3	-	AB893617
14 Shosambetsu	44°35′N/141°47′E	-	-	14-1	AB893807	AB893638
				14-2	AB893808	AB893639
16 Yagishiri Island	44°26′N/141°25′E	7	10	16-1	AB893824	AB893668
17 Yagishiri Island	44°26′N/141°25′E	3	-	17-1	AB893830	AB893679
				17-2	-	AB893678
18 Teuri Island	44°26′N/141°19′E	5	-	18-1	-	AB893680
				18-2	-	AB893681
19 Nishiokoppe	44°21′N/142°58′E	1	-	19-1	-	AB893614
20 Tomamae	44°20′N/141°40′E	3	4	20-1	-	AB893640
				20-2	-	AB893641
				20-3	-	AB893642
21 Horokanai	44°18′N/142°10′E	-	4	21-1	AB893833	AB893684
22 Fukinoue	44°12′N/143°01′E	-	-	22-1	-	AB893613
23 Tomamae	44°08′N/141°47′E	-	-	23-1	-	AB893669
				23-2	-	AB893670
24 Obira	44°07′N/141°39′E	3	1	24-1	AB893809	AB893643
				24-2	AB893810	AB893644
27 Rumoi	43°54′N/141°42′E	2	-	27-1	AB893811	AB893645
				27-2	-	AB893646
				27-3	-	AB893647
				27-4	-	AB893648
30 Kamikawa	43°43′N/142°58′E	-	-	30-1	-	AB893612
31 Kitami	43°39′N/143°15′E	1	2	31-1	AB893795	AB893610
				31-2	AB893796	AB893611
32 Hirano	43°20′N/142°21′E	6	-	32-1	AB893818	AB893657
				32-2	AB893819	AB893658
				32-3	AB893820	AB893659
				32-4	AB893821	AB893665
				32-5	-	AB893660
				32-6	-	AB893661
				32-7	-	AB893662
				32-8	-	AB893663
				32-9	-	AB893664
33 Bibai	43°19′N/141°58′E	-	1	33-1	-	AB893676
				33-2	-	AB893677
34 Bibai	43°19′N/141°57′E	1	1	34-1	AB893812	AB893649
				34-2	AB893813	AB893650
				34-3	-	AB893651
35 Bibai	43°19′N/141°52′E	4	3	35-1	-	AB893675
36 Shakotan	43°19′N/140°21′E	-	1	36-1	AB893840	AB893694
				36-2	-	AB893692
				36-3	-	AB893693
39 Yubari	43°03′N/142°06′E	2	2	39-1	AB893814	AB893652
				39-2	AB893815	AB893653
				39-3	-	AB893654
40 Ebetsu	43°02′N/141°31′E	-	-	40-1	AB893829	AB893674
41 Sapporo	42°59′N/141°06′E	1	-	41-1	AB893839	AB893691
44 Kuromatsunai	42°39′N/140°19′E	3	-	44-1	AB893828	AB893673
				44-2	AB893827	-
45 Shimamaki	42°37′N/140°06′E	1	1	45-1	AB893825	AB893671
				45-2	AB893826	AB893672
				45-3	AB893837	AB893689
				45-4	AB893838	AB893690
				45-5	-	AB893688
46 Oshamambe	42°35′N/140°13′E	-	-	46-1	AB893835	AB893687
				46-2	-	AB893686
48 Urakawa	42°13′N/142°58′E	9	2	48-1	AB893834	AB893685
49 Yakumo	42°11′N/140°06′E	-	-	49-1	AB893836	-
53 Samani	42°04′N/143°07′E	3	1	53-1	AB893816	AB893655
				53-2	AB893817	AB893656
Ezohelix gainesi						
5 Rebun Island	45°18′N/141°02′E	-	-	5-2	AB893856	AB893722
7 Rishiri Island	45°13′N/141°14′E	-	-	7-3	AB893854	AB893720
				7-4	AB893855	AB893721
10 Nakatombetsu	44°59′N/142°17′E	-	-	10-4	AB893852	AB893716
				10-5	AB893853	AB893717
				10-6	-	AB893718
				10-7	-	AB893719
11 Horonobe	44°55′N/142°00′E	-	-	11-3	AB893892	AB893765
				11-4	AB893894	AB893766
13 Esashi	44°46′N/142°30′E	-	-	13-4	-	AB893712
				13-5	-	AB893713
				13-6	-	AB893714

15	Okoppe	44°39′N/143°04′E	-	-	13-7	-	AB893715
					15-1	AB893851	AB893708
					15-2	-	AB893709
					15-3	-	AB893710
					15-4	-	AB893711
17	Yagishiri Island	44°26′N/141°25′E	-	-	17-3	AB893890	AB893762
					17-4	AB893889	-
18	Teuri Island	44°26′N/141°19′E	3	-	18-3	AB893891	AB893763
					18-4	AB893892	AB893764
19	Nishiokoppe	44°21′N/142°58′E	-	-	19-2	AB893850	AB893705
					19-3	-	AB893706
					19-4	-	AB893707
20	Tomamae	44°20′N/141°40′E	-	-	20-4	AB893857	AB893723
21	Horokanai	44°18′N/142°10′E	-	1	21-2	AB893895	AB893767
					21-3	AB893896	AB893768
					21-4	AB893897	AB893769
22	Takinoue	44°12′N/143°01′E	-	-	22-2	AB893848	AB893701
					22-3	AB893849	AB893702
					22-4	-	AB893703
					22-5	-	AB893704
23	Tomamae	44°08′N/141°47′E	-	-	23-3	AB893873	AB893747
					23-4	-	AB893746
24	Ubira	44°07′N/141°39′E	-	-	24-3	AB893858	AB893724
26	Takinoue	43°56′N/142°57′E	-	-	26-1	AB893847	AB893700
27	Kumoi	43°54′N/141°42′E	1	-	27-5	AB893859	AB893725
					27-6	AB893860	AB893726
					27-7	-	AB893727
					27-8	-	AB893728
28	Koshimizu	43°48′N/144°40′E	-	-	28-1	AB893843	AB893696
29	Mashike	43°47′N/141°40′E	-	-	29-1	AB893888	AB893761
					29-2	AB893887	-
30	Kamikawa	43°43′N/142°58′E	-	-	30-2	AB893846	AB893699
31	Kitami	43°39′N/143°15′E	-	-	31-3	AB893844	AB893697
					31-4	AB893845	AB893698
32	Urano	43°20′N/142°21′E	1	1	32-10	AB893863	AB893734
					32-11	AB893872	-
33	Bibai	43°19′N/141°58′E	1	1	33-3	AB893886	AB893759
					33-4	-	AB893760
34	Bibai	43°19′N/141°57′E	2	2	34-4	AB893861	AB893729
					34-5	AB893862	AB893730
					34-6	-	AB893731
35	Bibai	43°19′N/141°52′E	-	2	35-2	AB893885	AB893758
					35-3	AB893884	-
36	Shakotan	43°19′N/140°21′E	3	-	-	-	-
37	Shikaoi	43°18′N/143°07′E	-	-	37-1	AB893842	AB893695
38	Tomari	43°03′N/140°30′E	1	1	38-1	-	AB893732
39	Yubari	43°03′N/142°06′E	-	-	39-4	AB893864	AB893735
					39-5	AB893865	AB893736
40	Obetsu	43°02′N/141°31′E	23	7	40-2	AB893882	AB893756
					40-3	AB893883	AB893757
41	Sapporo	42°59′N/141°06′E	-	-	41-2	AB893905	AB893776
42	Nemuro	42°49′N/142°59′E	-	-	42-1	AB893841	-
43	Rusutsu	42°41′N/140°50′E	-	-	43-1	-	AB893733
44	Kuromatsunai	42°39′N/140°19′E	-	-	44-3	AB893881	AB893754
					44-4	-	AB893755
45	Shimamaki	42°37′N/140°06′E	-	-	45-6	AB893879	AB893753
					45-7	AB893880	-
46	Oshamambe	42°35′N/140°13′E	2	-	46-3	AB893899	AB893771
					46-4	AB893900	AB893772
47	Yukawa	42°33′N/141°58′E	-	-	47-1	AB893903	AB893774
					47-2	AB893904	AB893775
48	Urakawa	42°13′N/142°58′E	-	-	48-2	AB893898	AB893770
49	Yakumo	42°11′N/140°06′E	-	-	49-2	AB893901	-
					49-3	AB893902	AB893773
50	Akkushiri Island	42°10′N/139°30′E	-	-	50-1	AB893878	AB893752
51	Akkushiri Island	42°09′N/139°24′E	-	-	51-1	AB893877	AB893751
53	Samani	42°04′N/143°07′E	-	-	53-3	AB893866	AB893737
					53-4	AB893867	AB893738
					53-5	AB893868	AB893739
					53-6	-	AB893740
54	Kaminokuni	41°42′N/140°18′E	-	-	54-1	AB893874	AB893748
55	Matsumae	41°42′N/140°18′E	-	4	55-1	AB893875	AB893749
					55-2	AB893876	AB893750
56	Daisen, Akita	39°33′N/140°43′E	-	-	56-1	-	AB893741
57	Daisen, Akita	39°33′N/140°43′E	-	-	57-1	AB893869	AB893742
58	Yusa, Yamagata	39°06′N/140°00′E	-	-	58-1	AB893870	AB893743
					58-2	AB893871	AB893744
					58-3	-	AB893745
Karaftohelix blakeana							
1	Soya, Wakkanai	45°31′N/141°56′E	-	-	1-3	AB893911	AB893782
					1-4	AB893912	AB893783
					1-5	-	AB893784
4	Rebun Island	45°18′N/141°01′E	-	-	4-1	AB893908	AB893779
					4-2	AB893909	AB893780
					4-3	AB893910	AB893781
25	Rausu	44°02′N/145°08′E	-	-	25-1	AB893906	AB893777
					25-2	AB893907	AB893778
Panegista apoiensis							
52	Samani	42°06′N/143°01′E	-	-	52-1	AB893913	AB893788
					52-2	AB893914	AB893789
					52-3	AB893915	AB893790
					52-4	AB893916	AB893792
					52-5	-	AB893786
					52-6	-	AB893787
					52-7	-	AB893791
					52-8	-	AB893785
Panegista takahidei							
41	Sapporo	42°59′N/141°06′E	-	-	41-3	AB893917	AB893794
					41-4	-	AB893793
Total			115	57		123	185

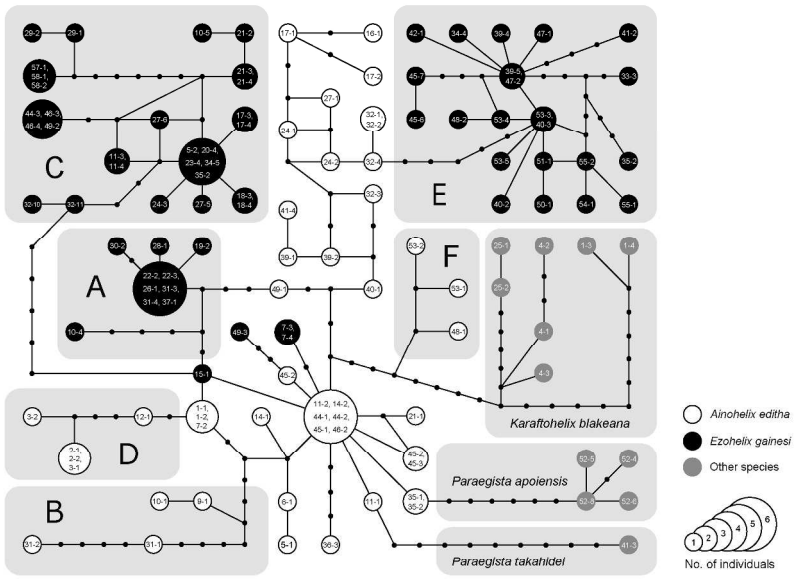

Appendix 2. The parsimony haplotype network conducted using the nDNA. Circles (nodes) indicate each haplotype. Numbers in the circles indicate the individual numbers shown in Appendix 1. Connection between nodes indicates a single character-state change. The empty nodes indicate missing haplotypes. Numbers in the nodes indicate the sampling location, and the size of the nodes is proportional to the haplotype's frequency. White and black nodes indicate haplotypes of Ainohelix editha, Ezohelix gainesi, respectively. Gray nodes indicate the other three species, Karaftohelix blakeana, Paraegista takahidei and P. apoiensis.
282x211mm (300 x 300 DPI)